

Grignard Reaction

Comprehensive Study of the Enhanced Reactivity of Turbo-Grignard Reagents**

Andreas Hermann, Rana Seymen, Lukas Brieger, Johannes Kleinheider, Bastian Grabe, Wolf Hiller, and Carsten Strohmann*

Abstract: Since its introduction in 2004, Knochel's so called Turbo-Grignard reagents revolutionized the usage of Grignard reagents. Through the simple addition of LiCl to a magnesium alkyl an outstanding increase in reactivity can be achieved. Though the exact composition of the reactive species remained mysterious, the reactive mixture itself is readily used not only in synthesis but also found its way into more distant fields like material science. To unravel this mystery, we combined single-crystal X-ray diffraction with in-solution NMR-spectroscopy and closed our investigations with quantum chemical calculations. Using such a variety of methods, we have gained insight into and an explanation for the extraordinary reactivity of this extremely convenient reagent by determining the structure of the first bimetallic reactive species [*t*-Bu₂Mg·LiCl·4thf] with two *tert*-butyl anions at the magnesium center and incorporated lithium chloride.

Since their first description by Phillippe Barbier and its further development by Victor Grignard, granting the latter the Nobel Prize in 1912, the compound class of organo-magnesium halides are still a subject of high and extensive scientific research.^[1] The usage of these compounds, known as Grignard reagents, expanded from simple electrophilic addition and halogen exchange reactions^[2] to precursors of more complex coupling reactions^[3] and even found their way into synthetically more distant fields like optoelectronics.^[4] For this reason, experimental and theoretical studies are conducted heavily to narrow down their

composition and structure and thereby understand and influence their widely used reactivity.^[5] More than 100 years after the first synthesis of Grignard reagents, Knochel et al. took these reagents to a whole new level. They discovered, that the addition of LiCl turns on the “turbo” and not only dramatically enhances their reactivity but also their chemoselectivity, especially towards Mg-halide exchanges.^[6] While an increase in yield and a decrease in reaction time could be observed, reaction conditions applied were milder and the functional group tolerance higher. Similar to the turbo-Grignard reagents the addition of LiCl to halo magnesium amides leads to the formation of turbo-Hauser bases with dramatically improved reactivities, chemoselectivities and functional group tolerances, in particular towards deprotonation reactions.^[7] In 2005, Knochel et al. also showed that through the addition of [15]crown-5 and thereby complexation of MgCl₂ the Schlenk equilibrium of *i*-PrMgCl·LiCl (**1a**) can be shifted towards the di-organo-magnesium species *i*-Pr₂Mg·2 LiCl (**3a**) which leads to even shorter reaction times and higher conversion rates (s. Scheme 1).^[8]

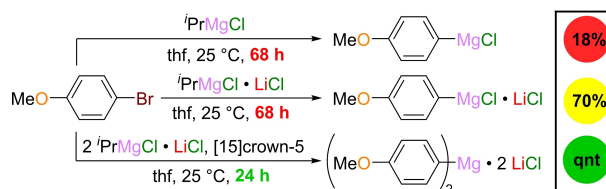
While examples for these reagents with their extraordinary properties are numerous, their constitution is not clear at all. When Schlenk introduced his fundamental concept, which is closely intertwined with Grignard reagents, he concluded rightfully that there is not only one defined but an equilibrium between different species.^[9] In fact there is a mixture of several aggregates which are all connected by equilibria (s. Scheme 2). The position of these equilibria depends not only on the organyl rest, but also on the applied solvent, the concentration, the temperature or the used halide and are subject to several experimental and quantum chemical investigations to “unravel this chemical puzzle”.^[10,11] In the case of the turbo-Grignard reagents, these equilibria are also affected by the added LiCl, thereby becoming more complex and making it even more difficult

[*] Dr. A. Hermann, R. Seymen, Dr. L. Brieger, J. Kleinheider, Prof. Dr. C. Strohmann
 Inorganic Chemistry, TU Dortmund University
 Otto-Hahn-Str. 6, 44227 Dortmund (Germany)
 E-mail: mail@carsten.strohmann.de

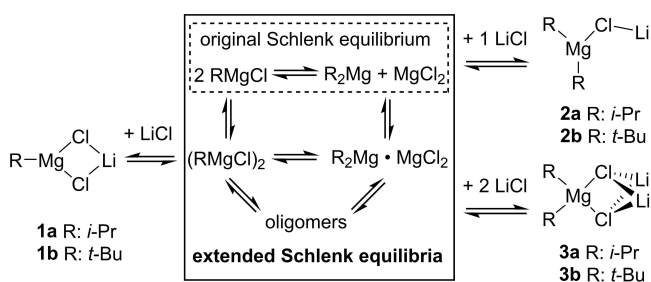
Dr. B. Grabe, Prof. Dr. W. Hiller
 Faculty of Chemistry and Chemical Biology, TU Dortmund University
 Otto-Hahn-Str. 4a, 44227 Dortmund (Germany)

[**] A previous version of this manuscript has been deposited on a preprint server (<https://doi.org/10.17877/DE290R-22376>).

© 2023 The Authors. Angewandte Chemie International Edition published by Wiley-VCH GmbH. This is an open access article under the terms of the Creative Commons Attribution License, which permits use, distribution and reproduction in any medium, provided the original work is properly cited.



Scheme 1. Acceleration of the Mg–Br-exchange of 4-bromanisole through the addition of LiCl or [15]crown-5 and LiCl to *i*-PrMgCl; the conversion of the reaction was determined by GC analysis on aliquots.^[6a,8]

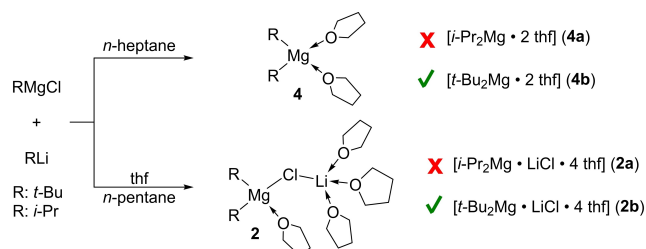


Scheme 2. Schlenk equilibria and tentative structural suggestions of different turbo-Grignard congeners.^[11,15]

to pin down and analyse reactive species. By using a combination of different experimental methods and quantum chemical calculations Stalke et al. were able to gain some insight into these underlying equilibria in ethereal solvents.^[12] Studies towards the solid-state structure of *i*-PrMgCl·LiCl lead to oligomeric structures incorporating four magnesium centers but are lacking LiCl.^[13] Yet, these studies can be seen as good examples for the diversity and high dynamic profile of the Schlenk equilibrium and its associated problem of finding defined and thereby characterizable species.^[14] Thus, the reactive species of **1**, **2** or **3** could never be clearly characterized, leading to different tentative structural suggestions of the reactive species.

Herein, we present the first study of such a reactive species with two separate alkyl anions, using single-crystal X-ray diffraction to determine the solid-state structure as well as ¹H-⁷Li-HOESY- in combination with ¹H-DOSY-NMR-spectroscopy to proof the existence of the found species in solution. Furthermore, we used these structures as a starting point to conduct quantum chemical calculations to explain the observed increase in reactivity upon addition of LiCl.

In contradiction to previous studies, we started our investigation on the other side of the equilibrium shown in Scheme 2 (right hand side). Therefore, we mixed *i*-PrMgCl with *i*-PrLi and *t*-BuMgCl with *t*-BuLi to see if we can obtain structural data of species **2** or **3**. While the crystallization attempts of the *i*-Pr species failed, we were able to crystallize two different *t*-Bu magnesium species (**4b** and **2b**, s. Scheme 3). We anticipate that the crystallization of the *i*-Pr species fails due to the higher mobility of the *i*-Pr compared to the *t*-Bu.



Scheme 3. Synthetic route to the pure di-organo-magnesium species **4a** and **4b** and the turbo-Grignard congeners **2a** and **2b**.

By mixing commercially available *t*-BuMgCl (in thf) and *t*-BuLi (in *n*-pentane), removing solvents and precipitating LiCl by recrystallizing the reagent mixture in *n*-heptane, we were able to obtain crystals of [*t*-Bu₂Mg·2thf] (**4b**). **4b** crystallizes in the monoclinic crystal system, space group *C2/c* (s. Figure 1) where the asymmetric unit contains half of the monomer of the di-organo-magnesium species **4b**. The magnesium center is coordinated by the two *t*-Bu ligands and two thf molecules. This coordination pattern is well known in the literature from other ethereal di-organo-magnesium compounds.^[16]

By simply mixing the two reagents *t*-BuMgCl and *t*-BuLi and storing the mixture over night at -80°C , we obtained colourless crystals. In addition to the usual high sensitivity of organometallic compounds to moisture and oxygen, these crystals proved to be very sensitive to slight temperature changes. While temperatures below 150 K (-123°C) resulted in shattering of the crystals caused by an irreversible phase transition, temperatures above 200 K (-73°C) resulted in melting. By using this sweet spot, we were able to determine the structure of, what we believe is a turbo-Grignard congener.

The compound [*t*-Bu₂Mg·LiCl·4thf] (**2b**) crystallizes in the monoclinic crystal system, space group *P2₁/c* (s. Figure 2). The asymmetric unit contains one magnesium center, which is coordinated by two *t*-Bu anions and one thf molecule in similar manner as in the structure of **4b**. The magnesium cation is connected via the chloride anion with the lithium cation, which is coordinated by three thf molecules. This R₂Mg–Cl–Li structural motif was previously obtained only by using a chelating dianion, resulting in a five-membered C–C–C–Mg ring, slightly shorter Mg–C distances of 2.143(2) Å and 2.132(2) Å as well as a much more acute C–Mg–C angle of about 88° compared to structure **2b**. In contrast to the referenced structure of Zhang et al., **2b** and **4b** feature Mg–C distances of about 2.18 Å and C–Mg–C angles of more than 120°, although it should be noted that these measurements were each performed at different temperatures.^[17]

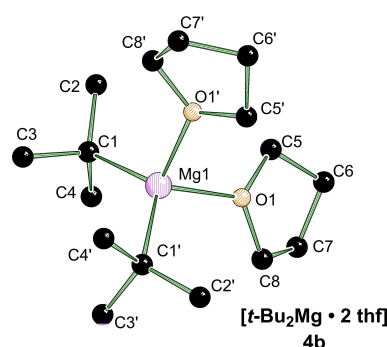


Figure 1. Molecular structure of [*t*-Bu₂Mg·2thf] (**4b**) in the crystal. Symmetry operation: $1-x, y, 3/2-z$. Small selection of bond lengths and angles: Mg1–C1 2.1765(11) Å, C1–Mg1–C1' 122.51(6)°. For further information on selected bond lengths and angles see Supporting Information Figure S5.

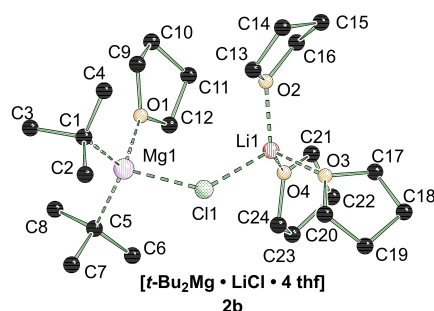
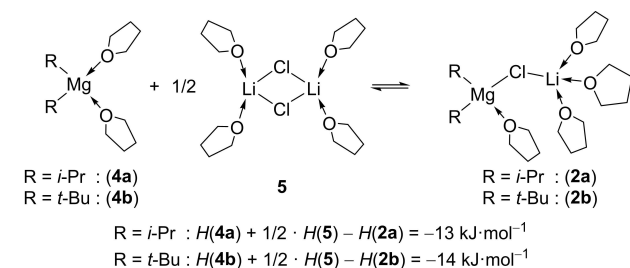


Figure 2. Molecular structure of $[t\text{-Bu}_2\text{Mg} \cdot \text{LiCl} \cdot 4\text{thf}]$ (**2b**) in the crystal. Small selection of bond lengths [Å] and angles [°]: Mg1–C1 2.176(2), Mg1–C5 2.183(2), Mg1–Cl1 2.4103(8), Li1–Cl1 2.302(3), C1–Mg1–C5 122.78(8), Mg1–Cl1–Li1 123.92(10). For further information on selected bond lengths and angles see Supporting Information Figure S13.

This leads to the question: Does the structural motif of **2b** found in the solid state also represent the general structure of these di-organo-magnesium-LiCl-adducts in solution? To answer this question, we used the found structural motifs of **4b** and **2b** as a basis for quantum chemical calculations of the equilibrium between **4a**, $[\text{LiCl} \cdot 2\text{thf}]_2$ (**5**) and **2a** and **4b**, **5** and **2b** (**5** is already characterized in solid state and solution^[13,18]).

The calculated enthalpy of formation of -13 kJ mol^{-1} (**2a**) and -14 kJ mol^{-1} (**2b**) shown in Scheme 4 is in clear favour of the LiCl adducts **2** over the separated species **4** and **5**. In a detailed quantum chemical calculation on the tentative structural suggestions of different turbo-Grignard congeners with $\text{R} = t\text{-Bu}$, as shown in Scheme 2, aggregate **2b** was found to be favored over the other congeners **1b** and **3b** (see Supporting Information p. S56).

Confident by these results, we moved from theory to experiment and conducted different NMR-experiments of a mixture of **4b** and **5** as well as of a mixture of *i*-PrMgCl with *i*-PrLi. By addition of **4b** to LiCl an upfield shift of about 0.6 ppm for the ^7Li -signal can be observed, pointing towards a change in coordination sphere of the lithium ion. When comparing the solution of **2a** with the solution of **5**, the same upfield shift, as previously recorded for **2b**, was observed. Furthermore, using ^1H - ^7Li -HOESY-NMR experiments, we were able to confirm a coupling between the protons of the carbanionic ligands (*t*-Bu **2b** and *i*-Pr **2a**) and



Scheme 4. Calculated ΔH of the equilibrium between the three species $[\text{R}_2\text{Mg} \cdot 2\text{thf}]$ (**4**), $[\text{LiCl} \cdot 2\text{thf}]_2$ (**5**) and $[\text{R}_2\text{Mg} \cdot \text{LiCl} \cdot 4\text{thf}]$ (**2**); M06-2X/6-311 + g(d,p), SMD-solvent model with thf as solvent.

the ^7Li -nucleus, proving thereby a formation of an aggregate containing both (see Supporting Information Figures S9 and S18). This led us to the question whether these aggregates also represent the found solid state structure of **2b**. To further pursue this question, we investigated the aggregate sizes of **2a** and **2b** by ^1H -DOSY-NMR experiments (s. Table 1). All diameters found in solution are in good agreement with either the diameter calculated by quantum chemical calculations (**2a**) or the one found in the solid-state (**2b**).

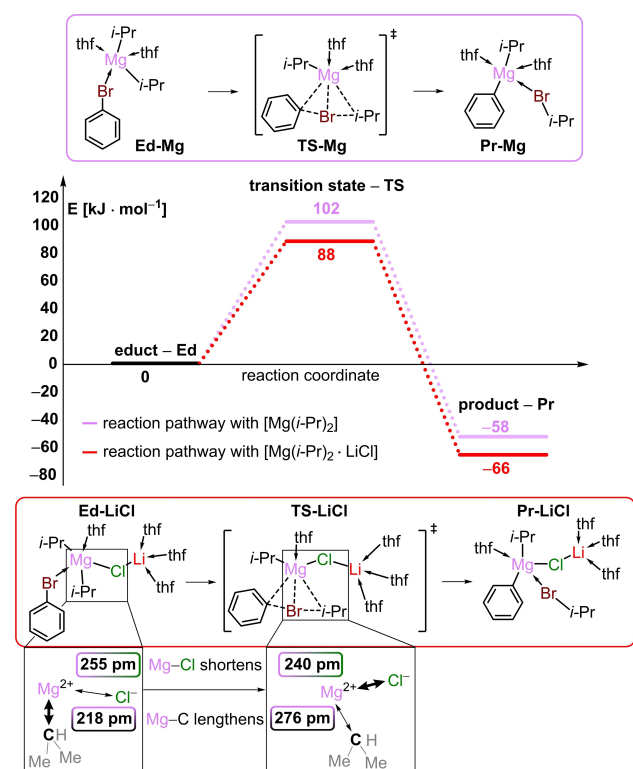
The found solid state structure of **2b** in combination with the employed NMR-experiments of **2a** and **2b** unearth a yet unnoticed reactive intermediate, which was not considered in mechanistic approaches so far. Therefore, we used this new structural motif to model a simple Br–Mg-exchange of bromobenzene with either $[i\text{-Pr}_2\text{Mg} \cdot 2\text{thf}]$ (**4a**) or $[i\text{-Pr}_2\text{Mg} \cdot \text{LiCl} \cdot 4\text{thf}]$ (**2a**) as reagent. Indeed, a barrier lowering effect of the incorporated lithium chloride known from various examples can be observed and understood through these quantum chemical calculations (s. Scheme 5).

Through the incorporation of a third anionic ligand ($2 i\text{-Pr}^- + \text{Cl}^-$) the highly charged and less coordinated magnesium cation is better stabilized in the transition state **TS-LiCl** than in **TS-Mg** (s. Scheme 5). This stabilization can be explained by a shortening of the distance between magnesium and chloride by more than 10 pm from **Ed-LiCl** to **TS-LiCl** and thereby elevating stabilizing coulomb interactions. At the same time, the higher polarity of the calculated LiCl-aggregates, especially in the case of the transition state, results in a higher sensitivity towards solvent effects. Thus, for a more accurate calculation, employment of a more sophisticated solvent model such as SMD is required. The values found hereby should not be over-interpreted as absolute statements but should be seen as trends pointing towards a direction (for a detailed discussion see Supporting Information p. S73). All these observations together provide an explanation why the addition and incorporation of LiCl enhances the reactivity of Grignard reagents in the experimental well-observed manner.

By starting off with the crystallization and characterization of a turbo-Grignard congener by single-crystal X-ray diffraction, we were lucky to get a grip on these otherwise highly dynamic intermediates. From this starting point we were able to corroborate the gained structural information as a thermodynamic minimum by quantum chemical calculations and as present in solution via multiple NMR experiments. Finally, we conducted quantum chemical calculations of a Mg–Br exchange, showing that the incorporation of LiCl indeed possesses a barrier lowering effect by stabilizing

Table 1: Experimental results of the ^1H -DOSY-NMR experiment of a 0.5 M solution of a 1:1 mixture of **4b** and **5**, and *i*-PrMgCl and *i*-PrLi in thf- d_6 conducted at room temperature.

compound	nucleus	shift	D [m^2/s]	d [nm]
2a	$[\text{CH}(\text{CH}_3)_2]$	–0.56 ppm	$7.43 \cdot 10^{-10}$	1.3
	$[\text{CH}(\text{CH}_3)_2]$	1.07 ppm	$7.56 \cdot 10^{-10}$	1.2
2b	$[\text{C}(\text{CH}_3)_3]$	0.82 ppm	$7.65 \cdot 10^{-10}$	1.2



Scheme 5. Calculated ΔH for the Br–Mg exchange of bromobenzene with $[i\text{-Pr}_2\text{Mg} \cdot 2 \text{ thf}]$ (**4a**) and $[i\text{-Pr}_2\text{Mg} \cdot \text{LiCl} \cdot 4 \text{ thf}]$ (**2a**); M06-2X/6-311 + g(d,p) with SMD-solvent model and thf as solvent; for further information see Supporting Information; calculated bond lengths at the stationary points **Ed-LiCl** and **TS-LiCl**.

the transition state of this reaction (s. Scheme 5). Most notably, our results thereby explain the enhanced reactivity of such mixed $\text{R}_2\text{Mg} \cdot \text{LiCl}$ reagents, as already proven by Knochel et al. (s. Scheme 1).^[8] Based on these findings, it should be discussed to which extent these di-organo species ($\text{R}_2\text{Mg} \cdot \text{LiCl}$) are also involved in the reactivity of the widely used turbo-Grignard reagents ($\text{RMgCl} \cdot \text{LiCl}$), in which they should be present due to the Schlenk equilibrium. Therefore, the in situ mixing of commercially available Grignard reagents with lithium alkyls should be reconsidered as a fast path to easily enhance the reactivity of Grignard reagents. Finally, the results presented here show why and how a general reactivity enhancement can be achieved by anionic components such as a simple chloride anion. By adding another piece to the turbo-Grignard puzzle, we hope that the results of our work will not only magnify the scientific picture of these high-performance reagents but also that of the influencing effects of anionic components. We hope that our findings will seed inspiration in other scientists for further improvement of organometallic reagents.

Acknowledgements

We thank the *Deutsche Forschungsgemeinschaft* (DFG, German Research Foundation, project number 452669591) for financial support. A. H. and R. S. thank the *Studien-*

stiftung des deutschen Volkes for a fellowship. L. B. and J. K. thank the *Fonds der Chemischen Industrie* (FCI) for a Kekulé Fellowship. Open Access funding enabled and organized by Projekt DEAL.

Conflict of Interest

The authors declare no conflict of interest.

Data Availability Statement

The data that support the findings of this study are available in the supplementary material of this article.

Keywords: Grignard Reaction · Metal-Halogen Exchange · Turbo-Grignard · X-Ray Diffraction

- [1] a) M. F. P. Barbier, *C. R. Hebd. Seances Acad. Sci.* **1899**, 128, 110; b) M. Zanda, *Synfacts* **2018**, 14, A153–A169; c) V. Grignard, *C. R. Hebd. Seances Acad. Sci.* **1900**, 130, 1322.
- [2] a) P. Vollhardt, N. Schore, *Organic Chemistry*, Macmillan Learning, New York, **2014**; b) Z. Rappoport, I. Marek, S. Patai, *The Chemistry of Organomagnesium Compounds*, John Wiley & Sons, Ltd, Chichester, UK, **2008**; c) G. S. Silverman, P. E. Rakita, *Handbook of Grignard Reagents*, CRC Press, **1996**; d) A. Desaintjean, T. Haupt, L. J. Bole, N. R. Judge, E. Hevia, P. Knochel, *Angew. Chem. Int. Ed.* **2021**, 60, 1513; e) A. S. Sunagatullina, F. H. Lutter, P. Knochel, *Angew. Chem. Int. Ed.* **2022**, 61, e202116625; f) C. Yeardeley, A. R. Kennedy, P. C. Gros, S. Touchet, M. Fairley, R. McLellan, A. J. Martínez-Martínez, C. T. O'Hara, *Dalton Trans.* **2020**, 49, 5257.
- [3] a) M. S. Kharasch, E. K. Fields, *J. Am. Chem. Soc.* **1941**, 63, 2316; b) R. J. P. Corriu, J. P. Mase, *J. Chem. Soc. Chem. Commun.* **1972**, 144a; c) K. Tamao, K. Sumitani, M. Kumada, *J. Am. Chem. Soc.* **1972**, 94, 4374; d) T. Scherpf, H. Steinert, A. Großjohann, K. Dilchert, J. Tappen, I. Rodstein, V. H. Gessner, *Angew. Chem. Int. Ed.* **2020**, 59, 20596; e) D. Posevins, A. Bermejo-López, J.-E. Bäckvall, *Angew. Chem. Int. Ed.* **2021**, 60, 22178.
- [4] T. P. Le, B. H. Smith, Y. Lee, J. H. Litofsky, M. P. Aplan, B. Kuei, C. Zhu, C. Wang, A. Hexemer, E. D. Gomez, *Macromolecules* **2020**, 53, 1967.
- [5] a) R. M. Peltzer, J. Gauss, O. Eisenstein, M. Cascella, *J. Am. Chem. Soc.* **2020**, 142, 2984; b) P. Schüler, H. Görls, S. Kriek, M. Westerhausen, *Chem. Eur. J.* **2021**, 27, 15508.
- [6] a) A. Krasovskiy, P. Knochel, *Angew. Chem. Int. Ed.* **2004**, 43, 3333; b) R. L.-Y. Bao, R. Zhao, L. Shi, *Chem. Commun.* **2015**, 51, 6884.
- [7] a) P. García-Álvarez, D. V. Graham, E. Hevia, A. R. Kennedy, J. Klett, R. E. Mulvey, C. T. O'Hara, S. Weatherstone, *Angew. Chem. Int. Ed.* **2008**, 47, 8079; b) D. R. Armstrong, P. García-Álvarez, A. R. Kennedy, R. E. Mulvey, J. A. Parkinson, *Angew. Chem. Int. Ed.* **2010**, 49, 3185.
- [8] A. Krasovskiy, B. F. Straub, P. Knochel, *Angew. Chem. Int. Ed.* **2005**, 45, 159.
- [9] a) W. Schlenk, W. Schlenk, *Ber. Dtsch. Chem. Ges. A* **1929**, 62, 920; b) D. Seyferth, *Organometallics* **2009**, 28, 1598.
- [10] a) J. Tammiku-Taul, P. Burk, A. Tuulmets, *J. Phys. Chem. A* **2004**, 108, 133; b) A. M. Henriques, A. G. H. Barbosa, *J. Phys. Chem. A* **2011**, 115, 12259; c) A. V. Tulub, V. V. Porsev in *NATO Science for Peace and Security Series A, Chemistry and*

- Biology* (Ed.: N. Russo), Springer Netherlands, Dordrecht, **2009**, pp. 385–397; d) M. B. Smith, W. E. Becker, *Tetrahedron* **1967**, *23*, 4215; e) R. Neufeld, T. L. Teuteberg, R. Herbst-Irmer, R. A. Mata, D. Stalke, *J. Am. Chem. Soc.* **2016**, *138*, 4796; f) S. Sakamoto, T. Imamoto, K. Yamaguchi, *Org. Lett.* **2001**, *3*, 1793; g) P. Sobota, B. Duda, *J. Organomet. Chem.* **1987**, *332*, 239.
- [11] R. M. Peltzer, O. Eisenstein, A. Nova, M. Cascella, *J. Phys. Chem. B* **2017**, *121*, 4226.
- [12] C. Schnegelsberg, S. Bachmann, M. Kolter, T. Auth, M. John, D. Stalke, K. Koszinowski, *Chem. Eur. J.* **2016**, *22*, 7752.
- [13] F. Blasberg, M. Bolte, M. Wagner, H.-W. Lerner, *Organometallics* **2012**, *31*, 1001.
- [14] S. D. Robertson, M. Uzelac, R. E. Mulvey, *Chem. Rev.* **2019**, *119*, 8332.
- [15] a) D. S. Ziegler, B. Wei, P. Knochel, *Chem. Eur. J.* **2019**, *25*, 2695; b) L. Shi, Y. Chu, P. Knochel, H. Mayr, *J. Org. Chem.* **2009**, *74*, 2760.
- [16] a) M. Arrowsmith, M. S. Hill, G. Kociok-Köhn, *Organometallics* **2010**, *29*, 4203; b) J. J. Sandoval, P. Palma, E. Álvarez, J. Cámpora, A. Rodríguez-Delgado, *Organometallics* **2016**, *35*, 3197; c) P. M. Scheetz, S. T. Chachula, R. P. Hughes, D. S. Glueck, C. E. Moore, M. Gembicky, A. L. Rheingold, *Organometallics* **2020**, *39*, 3802.
- [17] B. Wei, L. Liu, W.-X. Zhang, Z. Xi, *Angew. Chem. Int. Ed.* **2017**, *56*, 9188.
- [18] L. Knauer, C. Strohmann, *Chem. Commun.* **2020**, *56*, 13543.
- [19] Deposition numbers 2214771 (**4b**) and 2214772 (**2b**) contain the supplementary crystallographic data for this paper. These data are provided free of charge by the joint Cambridge Crystallographic Data Centre and Fachinformationszentrum Karlsruhe Access Structures service.

Manuscript received: February 20, 2023

Accepted manuscript online: March 27, 2023

Version of record online: May 8, 2023